УДК 550.31

FUNCTIONAL RENORMALIZATION PREDICTION OF RUPTURE

S. Gluzman[1], J. Andersen[1], D. Sornette[1,2]

[1] Laboratoire de Physique de la Matière Condensée CNRS UMR6622 and Université de Nice-Sophia Antipolis, Nice, France
[2] Institute of Geophysics and Planetary Physics and Department of Earth and Space Science University of California, Los Angeles, USA

We develop theoretical formulas for the prediction of the rupture of systems which are known to exhibit a critical behavior, based solely on the knowledge of the early time evolution of an observable, such as the acoustic emission rate as a function of time or of stress. From the parameterization of such early time evolution in terms of a low-order polynomial, we use the functional renormalization approach introduced by Yukalov and Gluzman to transform this polynomial into a function which is asymptotically a power law. The value of the critical time t_c, *conditioned* on the assumption that t_c exists, is thus determined from the knowledge of the coefficients of the polynomials. We test with success this prediction scheme with respect to the order of the polynomials and as a function of noise.

РЕНОРМАЛИЗАЦИЯ ПРОГНОЗА

С. Глузман[1], Д. Андерсен[1], Д. Сорнет[1,2]

[1] Лаборатория физики твердого тела Национального центра научных исследований и Университет Ниццы-София Антиполис, Ницца, Франция
[2] Калифорнийский университет в Лос Анджелесе, Институт физики Земли и планет и Департамент геофизики и космических исследований, Лос Анджелес, США

Выводятся теоретические формулы для прогноза разрыва в системах с критическим поведением. Формулы предполагают знание лишь ранней эволюции во времени наблюдаемой величины, напрмер, интенсивности акустической эмиссии в зависимости от времени или напряжения. Параметризуя такую раннюю эволюцию во времени с помощью полинома низкого порядка, мы используем подход функциональной параметризации, введенной Юкаловым и Глузманом, чтобы преобразовать этот полином в функцию, которая асимптотически является степенной. Таким образом, значение критического времени t_c, при условии, что t_c существует, определяется из знания коэффициентов полинома. Данная схема прогноза успешно проверена по отношению к порядку полинома и в зависимости от шума.

Introduction

To what extent can the material failure of a mechanical system under stress be forecasted? This question has enormous technological interest for its economic and human consequences, especially in the automobile, naval, aeronautics and space industries [1], as well as in the sensitive chemical and nuclear industries to cite a few among many examples.

If rupture occurs brutally without precursors, prediction is impossible. In contrast, Mogi noticed that, for experiments on a variety of materials, the larger the heterogeneity of the material, the stronger and more useful are the precursors to rupture [2]. For a long time, the Japanese research effort for earthquake prediction and risk assessment was based on this very idea [3].

These empirical facts have been put on a firm theoretical basis by using various simplified mechanical models of failure of heterogeneous materials which showed that, increasing the disorder changes rupture from first-order (abrupt) to critical (continuous with power-law properties) [4]. By the term "disorder', we refer to heterogeneity in material properties (elastic coefficients and rupture thresholds)

as well as inhomogeneous pre-stresses. In the presence of long-range elasticity, disorder is found to be always relevant leading to a critical rupture. However, the disorder controls the width of the critical region [5]. The smaller it is, the smaller will be the critical region, which may become too small to play any role in practice.

The potential for predicting rupture thus seems associated with its critical nature. Let us first review past works which support this concept of critical rupture. Theoretically, the concept that rupture is critical was first formulated by Vere-Jones [6] using critical branching models and Allègre et al. [7] using the percolation model and real-space renormalization group (see [8] for a general presentation). The Russian school has also extensively developed this concept [9–11]. One of us and co-workers have introduced a statistical two-dimensional model of dynamically evolving damage [12], which exhibits the critical time-to-failure dependence of the energy released up to the rupture. Based on a precise numerical description of the many growing interacting micro-cracks with a spatio-temporal organization which is a function of the stress-dependent damage law, one finds that, under a step-function stress loading, the total rate of damage increases on average as a power-law of the time-to-failure. In this model, rupture is a "critical point" in the statistical physics sense [8] and occurs as the culmination of the progressive nucleation, growth and fusion between microcracks, leading to a fractal network of cracks. This simple model has since then been found to describe quantitatively the experiments on the electric breakdown of insulator-conducting composites [13] and the damage by electromigration of polycrystalline metal films [14]. This led to the proposal and the empirical test on real engineering composite structures that failure in fiber composites is a genuine "critical" point [15]. This critical behavior may correspond to an acceleration of the rate of energy release or to a deceleration, depending on the nature and range of the stress transfer mechanism and on the loading procedure. A generalization is to extend the power-law behavior of the time-to-failure analysis by including corrections in the form of log-periodic modulations [15]. Log-periodicity is the hallmark of a hierarchy of discrete characteristic scales in the rupture process. Mathematically, it corresponds to adding an imaginary part to the exponent z (defined below). Intuitively, the log-periodic oscillations are oscillations that are periodic in the logarithm of the time-to-failure and thus corresponds to an accelerating frequency modulation as the critical time is approached. This acceleration of alternating ups and downs accounts for the succession of damage and quiescent phases self-organizing and culminating in the rupture.

Following this work [15], this method has been used extensively by the French Aerospace company Aérospatiale on pressure tanks made of kevlar-matrix and carbon-matrix composites used on the European Ariane 4 and 5 rockets. In this application, the method consists in recording acoustic emissions under constant stress rate. The acoustic emission energy as a function of stress is fitted by the critical theory mentioned above. One of the parameters is the time of failure and the fit thus provides a "prediction" when the sample is not brought to failure in the first test. The results indicate that a precision of a few percent in the determination of the stress at rupture is typically obtained using acoustic emission recorded about 20% below the stress for rupture. We now have a better understanding of the conditions, the mathematical properties and physical mechanisms at the basis of log-periodic structures [16].

The numerical simulations of Sahimi and Arbabi [17] have confirmed that, near the global failure point, the cumulative elastic energy released during fracturing of heterogeneous solids with long-range elastic interactions exhibit a critical behavior with observable log-periodic corrections. Molecular dynamics simulations of the geometry of fracture patterns in a dilute elastic network give similar results [18]: under a uniform strain which drives the fracture to develop by the growth and coalescence of the vacancy clusters in the network, there exists a characteristic time at which a dynamical transition occurs with a power law divergence of the average cluster size. The cluster growth near the critical time also exhibits spatial scaling in addition to the temporal scaling, namely as fracture develops with time, the connectivity length of the clusters increases and diverges at t_c. Recent experiments on the rupture of fiber-glass composites have also confirmed the critical scenario [19]. Johansen and Sornette [20] have recently re-analyzed the acoustic emissions recorded during the pressurization of spherical

tanks of kevlar or carbon fibers impregnated in a resin matrix wrapped up around a thin metallic liner (steel or titanium) fabricated and instrumented by Aerospatiale-Matra Inc. These experiments were performed as part of a routine industrial procedure, which tests the quality of the tanks prior to shipment. It was found that the seven acoustic emission recordings of seven pressure tanks which was brought to rupture exhibit clear acceleration in agreement with a power-law "divergence" expected from the critical point theory.

At the same time, it became tempting [21] to apply similar considerations to earthquakes. Indeed, over the years there has been a growing evidence that a significant proportion of large and great earthquakes are preceded by a period of accelerating seismic activity of moderate-sized earthquakes. These moderate earthquakes occur during the years to decades prior to the occurrence of the large or great events and over a region much larger than its rupture zone. Sornette and Sammis [21] identified a specific measurable signature of this criticality in terms of a power-law acceleration of the Benioff strain previously interpreted as an exponential mechanical-damage rate [22,23]. The combined observational and simulation evidence now seems to confirm that the period of increased moment release in moderate earthquakes signals the establishment of long-wavelength correlations in the regional stress field. Large or great earthquakes appear to dissipate a sufficient proportion of the accumulated regional strain to destroy these long wavelength stress correlations [24]. They can thus be considered as different from smaller earthquakes. According to this model, large earthquakes are not just scaled-up version of small earthquakes but play a special role as "critical points" [25,26]. Recent extensions to the intermediate scale of rockbursts in deep mines confirm the picture [27].

To summarize these works, there is a rather strong evidence that rupture in heterogeneous media is critical in the sense of statistical physics [8]. To what extent can the critical rupture concept be used to predict rupture? Voight noticed in an exciting precursory work that many systems fail by exhibiting a typical relationship relating the second time derivative $d^2\Omega/dt^2$ of some observable Ω to a positive power of Ω itself [28,29]. He then used this relationship to attempt predictions of failures in various materials and of volcanic eruptions. Basically, the relationship he postulates is nothing but a power law time-to-failure evolution of the observable Ω

$$\Omega(t) \;=\; A\,(t_c - t)^z, \tag{1}$$

where t_c is the critical time of rupture, z is a critical exponent and A a numerical amplitude. By differentiating twice and eliminating time, we indeed get $d^2\Omega/dt^2 = B\;\Omega^{(z+2)/z}$, where $B = z(z+1)A^{-2/z}$.

As we said above, the critical rupture concept establishes theoretically the law (1) as the result of the cooperative organization of precursory damage preparing the global rupture. If an observable such as the rate of acoustic emissions radiated during loading exhibit an acceleration close to rupture of form (1) as documented in several experiments [15,19,20] it is clear that one can try to fit the data by (1) and get a prediction from the determination of t_c.

In practice, the problem is that the fit of a simple power law (1) to a noisy data is rather unstable, so much so that often no fits can be found [30]. The problem comes from the fact that only close to t_c (in some relevant time units) can the power law be clearly distinguished from other parametric accelerating functional forms, such as an exponential. As an exponential has no critical time, this leads to an ill-defined rupture time. The fundamental limitation in using this prediction scheme is thus that t_c is determined only when data is used up to very close to t_c. This is thus far from the prediction goal to infer t_c from a distance! One possibility to improve the reliability and range of power law fits far from t_c has been proposed, based on log-periodic corrections to power laws [15,16,20,21,27].

In the present paper, we propose a different approach to the prediction of t_c. In the next section, we give the gist of the method and formulate the problem in precise terms. We also provide a brief summary of the functional renormalization method. In section 3, we test the method in the situation where both the polynomial expansion at early times and the value of t_c is known, to see how the time-dependence is reconstructed by the functional renormalization. In section 4, we present the

genuine prediction scheme which determines t_c solely from the knowledge of the first few coefficients of the polynomial fit at early times and the assumption that the late time dynamics is of the power law form (1). In particular, we test how the precision of the prediction improves by adding more terms in the polynomial expansion. Section 5 presents numerical tests of our method compared to direct fits by a power law for noisy data and section 6 concludes.

1. Formulation of the problem and outline of the method

The gist of the method is as follows. We assume that we are able to parameterize the early time evolution of an observable, such as the acoustic emission rate as a function of time or of stress by fitting the data to a low-order polynomial $\Omega(t) = a_0 + a_1 t + a_2 t^2 + \dots$. We then use the sophisticated functional renormalization approach introduced by Yukalov and Yukalov and Gluzman [31–42]. We use the version developed in [38] that transforms a polynomial into an analytic effective sum with an asymptotic power law of the form (1) close to some t_c to be determined. The value of the critical time t_c, *conditioned* on the assumption that t_c exists, is thus determined from the knowledge of the coefficients $a_0, a_1, a_2, \dots$.

In order to test our proposed scheme, we compare the results of our method to the exact evolution with time of the macroscopic crack length in an exactly solvable model of rupture with damage [43, 44]. In this self-consistent theory, the growth of a single macroscopic crack is controlled by cumulative damage dependent on stress history. The damage D accumulates according to the equation $dD/dt \propto \sigma^m$, where σ is the local stress proportional to the globally applied stress σ_0 but which takes into account the distortion due to the crack and m is the damage exponent. The law describing the growth of the crack, i.e., the dynamics of its half-length $a(t)$, is obtained from the following self-consistent condition: the time it takes from a point at the some distance L from the crack tip at time τ for its damage to reach the rupture threshold D^* is exactly equal to the time taken for the crack to grow from its size at time τ by an increment L so that its tip reaches the point exactly when it ruptures. For $m = 1$, the full solution is known [43, 44]

$$a(t) = \frac{a_0}{\cos(\pi\sigma_0 t/3D^*)}, \tag{2}$$

and is indeed of the form (1) close to $t_c = 3D^*/2\sigma_0$ with $z = -1$.

For the convenience of notations, we work in the sequel with dimensionless variables $f = a/a_0$ and $t\pi\sigma_0/(3D^*) \to t$, so that the solution (2) becomes

$$f_{\text{exact}}(t) = \frac{1}{\cos t}. \tag{3}$$

Let us assume that we have access only to the small time dynamics, captured mathematically by the first terms in the expansion of the solution (3):

$$f_a(t) = 1 + a_1 t^2 + a_2 t^4 + a_3 t^6 + \dots \qquad \text{with } a_1 = 1/2,\ a_2 = 5/24, \qquad \text{and } a_3 = \frac{61}{720}. \tag{4}$$

Since the cosine function is even in t, only even powers of t are present. Knowledge of only the first few terms in (4) is the relevant situation for instance in an experiment in which the early acoustic emissions are recorded and one would like to infer the subsequent evolution.

To make this paper self-consistent, we first outline the method we use, which is a direct adaptation of [38]. The complete mathematical foundation can be found in earlier publications [31–42]. Assume that we are interested in a function $\varphi(x)$ of a real variable x. Let perturbation theory give for this function the perturbative approximations $p_k(x)$ with $k = 0, 1, 2, \dots$, enumerating the approximation order. Define the algebraic transform $F_k(x, s) = x^s p_k(x)$. This transform changes the powers of the series $p_k(x)$, thus changing its convergence properties. As a result, the approximation order effectively increases from k to $k+s$. The inverse transform is $p_k(x) = x^{-s} F_k(x, s)$. Define the expansion function

$x = x(f,s)$ by the equation $F_0(x,s) = f$, where F_0 is the first available approximation and f is a new variable. Substituting $x(f,s)$ back to F_k, we get $y_k(f,s) = F_k(x(f,s),s)$. The transformation inverse to the latter reads $F_k(x,s) = y_k(F_0(x,s),s)$.

Consider the family $\{y_k\}$ as a dynamical system in discrete time k, the order of the approximations. The trajectory $\{y_k(f,s)\}$ of this dynamical system is, by construction, bijective to the approximation sequence $h\{F_k(x,s)\}$. This system can thus be called the approximation cascade. The next step is to embed the discrete sequence $\{y_k(f,s)\}$ into a continuous sequence $\{y(\tau,f,s)\}$ with $\tau \in [0,+\infty]$. Thus, the family $\{y(\tau,f,s) : \tau \in [0,+\infty]\}$ composes a dynamical system with continuous time, whose trajectory passes through all points of the approximation cascade trajectory. Such a system can thus be called the approximation flow. The evolution equation for a flow can be presented in the functional form $y(\tau+\tau',f,s) = y(\tau,y(\tau',f,s),s)$. We call this equation the self-similarity relation, which is the central concept of our approach. In this framework, the motion occurs in the space of approximations, where self-similarity is a necessary condition for convergence as a function of "time" defined as the approximation number. The evolution equation for the approximation flow can be rewritten in the differential form and then integrated over time between k and some k^*. The point k^* is to be chosen to provide the best approximation $F^*_{k+1}(x,s) = y(k^*,F_0(x,s),s)$ for the minimal time $k^* - k$. The cascade velocity $v_k(y,s)$ in the vicinity of the time k may be presented by the Euler discretization of the flow velocity giving $v_k(f,s) = V_k(x(f,s),s)$, with $V_k(x(f,s),s) = F_{k+1}(x,s) - F_k(x,s)$. The integral form of the evolution equation is

$$\int_{F_k}^{F^*_{k+1}} \frac{df}{v_k(f,s)} = k^* - k, \tag{5}$$

where $F_k = F_k(f,s)$ and $F^*_{k+1} = F^*_{k+1}(x,s)$. The approximation F^*_{k+1} must be reached during the minimal time. When no additional constraints are imposed, then the minimal time corresponds, evidently, to one step: $k^* = k+1$. Finding $F^*_k(x,s)$ from (5) and using the inverse transform leads to the self-similar approximation $p^*_k(x,s) = x^{-s}F^*_k(x,s)$.

Now, by means of the substitution $s \to s_k$, we have to introduce control functions s_k which can govern the convergence of the sequence $\{p^*_k(x,s_k)\}$. Following the standard procedure [31–42] and similar to the steps described above, we may construct an approximation cascade with its corresponding cascade velocity. Convergence of an approximation sequence is, in the language of dynamical theory, the same as the existence of an attracting fixed point for the corresponding approximation cascade. If the cascade trajectory tends to a fixed point, this means that the flow velocity goes to zero as "time" k goes to infinity. In practice, we cannot, of course, reach the limit $k \to \infty$, and have to stop at a finite (approximation order) k. Then, the condition to be as close to a fixed point as possible is the minimum of the velocity.

After the control functions are found from the minimal-velocity condition, we substitute them into p^*_k and obtain the final expression $f^*_k = p^*_k(x,s_k(x))$ for the self-similar approximation of the sought function. The practical way of using the minimal-velocity condition is to express it as a minimal difference condition. To check whether the obtained sequence $\{f^*_k(x)\}$ converges, we have to analyze whether the corresponding mapping is contracting. The mapping related to the sequence $\{f^*_k\}$ is constructed in the standard way [31–42] and the contraction, or stability, is analyzed by calculating the mapping multipliers. Ref. [38] has shown how this method of algebraic self-similar renormalization works to obtain accurate estimations of the critical behavior of a large variety of physical systems, starting from virial-type or perturbation expansions containing only second-order terms and derived for a region far from the critical point.

In the sequel, we translate this formalism to the case where x is now a real time, k is the order of the polynomial fit to the early time of the signal which plays also the role of "time" for the dynamical flow in the functional space. The goal is to describe as accurately as possible the finite-time singularity, which is equivalent to a critical point in the time domain. Before investigating the predictive power of our approach, we first investigate the possibility of reconstructing as faithfully as possible the time evolution based on the knowledge of the singularity.

2. Reconstruction of the crack dynamics from the knowledge of the small time dynamics and the position of a finite-time singularity

Here, we assume in addition that we know the position of the singularity at $t = \pi/2$ and its exponent, i.e., that

$$f(t) = \frac{1}{\pi/2 - t} \qquad \text{for} \quad t \to \pi/2 \ . \tag{6}$$

Note that the amplitude A of the pole is exactly equal to 1. We apply the Yukalov-Gluzman technique in its version related to crossover phenomena [39–42], to obtain the best approximation of $f(t)$ for arbitrary times based only on the knowledge (4) at small times and (6) at times close to rupture.

2.1. Using only $f_a(t) = 1 + a_1 t^2$ and (6)

From the expansion $f_a(t) = 1 + a_1 t^2$, the Yukalov-Gluzman method allows us to build the approximant

$$f_1^*(t) = \left[\left(\exp\left(a_1 t^2\right) \right)^{-\frac{1}{\beta}} + bt^4 \right]^{-\beta} ,$$

with two unknown parameters b and β, to be determined solely by demanding the existence of a crossover. The exponent β is determined from the condition that $f_a(t) = 1 + a_1 t^2$ must cross-over to (6). This gives $\beta = 1$ for the simple pole (6). The coefficient b is obtained from the condition of a pole at the known critical point $t_c = \pi/2$, which reads $1/f_1(t_c) = 0$. Solving for b, we finally get the first-order approximant

$$f_1^*(t) = \left[\exp\left(-a_1 t^2\right) - \frac{t^4}{t_c^4} \exp\left(-a_1 t_c^2\right) \right]^{-1} . \tag{7}$$

This approximant gives an amplitude $A_1 = 0.834$ for the simple pole, only 17% off the exact value $A = 1$. Fig. 1 plots in logarithmic scale the relative errors between the approximant f_1 and the exact expression (3) as a function of time t.

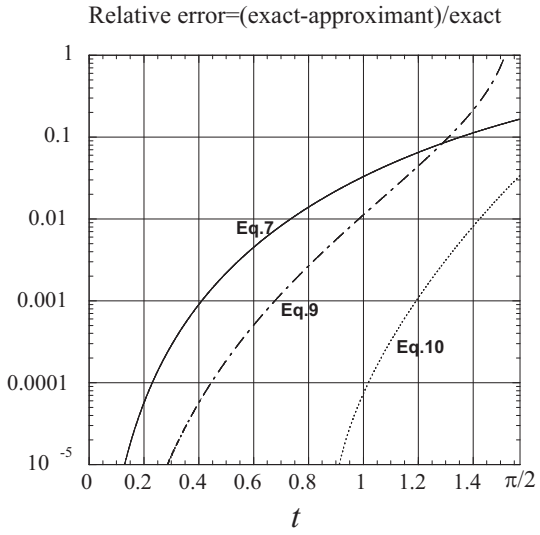

Fig. 1. Relative error $\left[f_{\rm exact}(t) - f_i^*(t)\right] / f_{\rm exact}(t)$, for the three approximation formulas: (7) for $f_1^*(t)$, (9) for $f_2^*(t)$, and (10) for $f_3^*(t)$, where $f_{\rm exact}(t)$ is given by (3).

2.2. Using $f_a(t) = 1 + a_1 t^2 + a_2 t^4$ and (6)

A similar procedure as in the previous case gives the second-order approximant

$$f_2^*(t) = \left[\exp\left(-a_1 t^2 \exp\left(\frac{a_2}{a_1} t^2 \right) \right) - \frac{t^6}{t_c^6} \exp\left(-a_1 t_c^2 \exp\left(\frac{a_2}{a_1} t_c^2 \right) \right) \right]^{-1} . \tag{8}$$

This second-order approximant can be improved by introducing an additional control parameter τ (optimal effective time $k^* - k$) such that we can enforce the condition that the coefficient a_2 is preserved in the renormalization procedure. In other words, the expansion of $f_2(t)$ is now imposed to have the same coefficient of its power t^4. The expression (8) is thus modified into

$$f_2^*(t) = \left[\exp\left(-a_1 t^2 \exp\left(\frac{a_2}{a_1}\tau\ t^2\right)\right) - \frac{t^6}{t_c^6}\exp\left(-a_1 t_c^2 \exp\left(\frac{a_2}{a_1}\ \tau\ t_c^2\right)\right)\right]^{-1}. \qquad (9)$$

The amplitude of the simple pole predicted by this approximant is found equal to 0.898, only 10% off from the exact value 1. The condition that the coefficient of the power t^4 in the expansion of (9) is equal to $a_2 = 5/24$ given by (4) leads to the improved second approximant of the form (9) with

$$\tau = 1 - \frac{a_1^2}{2a_2}.$$

Fig. 1 plots in logarithmic scale the relative errors between the approximant f_2 and the exact expression (3) as a function of time t.

2.3. Using $f_a(t) = 1 + a_1 t^2 + a_2 t^4 + a_3 t^6$ and (6)

An extension one step further in the Yukalov-Gluzman procedure gives

$$f_3^*(t) = \left[\left(\exp\left(a_1 t^2 \exp\left(\frac{a_2}{a_1} t^2 \tau_1 \exp\left(\frac{a_3}{a_2} t^2 \tau_2\right)\right)\right)\right)^{-\frac{1}{\beta}} + a_8 t^8\right]^{-\beta},$$

where the two control parameters τ_1 and τ_2 are to be determined from the condition that a_2 and a_3 are conserved by the renormalization. We find

$$\tau_1 = 1 - \frac{a_1^2}{2a_2}$$

and

$$\tau_2 = -\frac{1}{a_3\tau_1}\left(\frac{a_2^2\tau_1^2}{2a_1} + a_1 a_2 \tau_1 + \frac{a_1^3}{6} - a_3\right).$$

The coefficient a_8 is found from the condition on the critical point:

$$a_8 = -\frac{1}{t_c^8}\exp\left(-\frac{a_1}{\beta} t_c^2 \exp\left(\frac{a_2}{a_1} t_c^2 \tau_1 \exp\left(\frac{a_3}{a_2} t_c^2 \tau_2\right)\right)\right).$$

The solution then reads

$$f_3^*(t) = \left[\exp\left(-\frac{1}{2}t^2 \exp\left(\frac{1}{6}t^2 \exp\left(\frac{11}{60}t^2\right)\right)\right) - 256\left(\frac{t}{t_c}\right)^8 \exp\left(-\frac{\pi^2}{8}\exp\left(\frac{\pi^2}{24}\exp\left(\frac{11\pi^2}{240}\right)\right)\right)\right]^{-1}. \qquad (10)$$

This approximant gives an amplitude $A_3 = 0.9661$ for the simple pole, only 3.4% off the exact value $A = 1$. The quality of the reconstruction of the full function (3) can also be checked by comparing the exact value of the next term $(277/8064)\ t^8 = 0.03435\ t^8$ in the expansion (4) of the function (3). We find $0.034497\ t^8$, corresponding to an error of 0.4%.

Fig. 1 plots in logarithmic scale the relative errors between the approximants f_1^*, f_2^* and f_3^* and the exact expression (3).

3. Prediction of the critical time from the knowledge of the small time dynamics

We now assume the knowledge of the expansion (4) up to some order, representing for instance the experimental recording of an acoustic emission signal up to some stress level. In addition, we assume *only* the existence of a singularity of the form $1/(t_c - t)^K$ at some value t_c, using the insight from the theory of critical rupture, but do not know a priori neither the position of t_c, nor the value of the exponent K. In other words, we assume that we know that the system is bound to break but we do not know when and how. Our goal is to attempt to determine the critical time and the functional form of the signal on the approach to the critical rupture time from the recording of the early signals.

3.1. Standard approach from Yukalov and Gluzman [38]

Consider an expansion of some function φ in powers of some variable u given by

$$p_k(u) = \sum_{k=0}^{k} b_k \; u^k, \qquad \text{with} \quad b_0 = 1.$$

The method of algebraic self-similar renormalization [36–38] gives the following general recurrence formula for the approximant of order k as a function of the expansion $p_{k-1}(u)$ up to order $k-1$:

$$\varphi_k^*(u) = p_{k-1}(u) \left[1 - \frac{k \; b_k}{s} \; u^k \; p_{k-1}^{k/s}(u) \right]^{-s/k} \equiv \left[p_{k-1}^{-k/s}(u) - \frac{k \; b_k}{s} \; u^k \right]^{-s/k}, \tag{11}$$

where, generally speaking, $s = s_k(u)$, depends on the approximation number and the variable u.

First, let us estimate the position of the critical point. Using only $f_1(t) = 1 + a_1 t^2$, we can write it as the inverse of a function that is requested to vanish in order to obtain the singularity. Expanding in powers of t up to first order in t, we get the estimation $t_{c1} = \sqrt{2} = 1.414$, which should be compared with the exact value $\pi/2 = 1.571$. Including the next order from the expansion of $\cos(t)^{-1}$ leads to the improved estimate $t_{c2} = 1.59$.

Let us now obtain the expansion which will be used as a raw material for renormalization. Including the next order in $f_2(t) = f_1(t) + a_2 t^4$, inverting it, and expanding in powers of t up to t^4-terms, we obtain an expansion $p_2(t)$ for $1/f_2$:

$$p_2(t) = \sum_{k=0}^{2} b_k t^{2k}$$

$$b_0 = 1, \quad b_1 = -1/2, \quad b_2 = 1/24,$$

Note that, in the initial series, all coefficients in the expansion of cos^{-1} are positive, giving the worst possible case for resummation. In contrast, the coefficients of the inverted series have alternating signs, which may be better for resummation [38]. Hereafter, we apply the resummation procedure to the function $F \equiv 1/f$ inverse of f. Correspondingly, $f^* \equiv (1/F)^*$.

In order to determine the exponent K, we follow Yukalov and Gluzman [38] and construct the two approximants available from the knowledge of the two coefficients a_1 and a_2. They can be readily obtained from the general formula (11), with $u = t^2$. The first order approximant is

$$F_1^*(t) = \left(1 - \frac{b_1}{s_1} t^2 \right)^{-s_1}. \tag{12}$$

Representing $p_2(t)$ as $p_2(t) = 1 + b_1 t^2 (1 + (b_2/b_1) t^2)$, and applying the general formula to the expression in brackets, we obtain the second order approximant

$$F_2^*(t) = 1 + b_1 t^2 \left(1 - \frac{b_2}{b_1 s_2} t^2 \right)^{-s_2}. \tag{13}$$

Assume further that

$$s_1 = s_2 = s, \tag{14}$$

where s is a single control parameter, i.e. the limit of the total control function in the critical point, which will play the role of the critical index K. As it was explained in [38], such an assumption is well justified in the vicinity of a stable fixed point.

We impose the condition of the existence of a critical point, which delivers two equations for t_c and s:

$$F_1^*(t_c, s) = 0 \qquad \text{and} \qquad F_2^*(t_c, s) = 0. \tag{15}$$

The condition of maximum stability of the renormalization amounts to imposing that the difference $F_2^* - F_1^*$ be a minimum with respect to the set of parameters. The minimization of the difference is automatically satisfied when (15) holds, since the difference reaches its smallest possible value, namely zero.

The vanishing of F_1^* given by (12) gives $t_c^2 = s/a_1$. The second condition $F_2^* = 0$ with (13) yields the estimation $s = 1.258$ for the critical index, only 26% off the true value equal to 1. The critical time is given numerically by $t_c = 1.586$, very close to the exact value $\pi/2 = 1.5708$. Note that, as is often found in critical phenomena, an error of less than 1% in the location of the critical point is associated with a much larger error of about 26% on the exponent. In the scheme presented above, it was possible to find s and t_c from separate equations.

Such convenience does not hold for another approximation scheme, presented below, which has however other advantages such as simplicity. In order to separate the variables, we need an initial guess either for s or for t_c. Such an initial guess is provided naturally by the analog of a mean-field approximation.

3.2. Alternative approach: expansion around a "mean-field" approximation

Expansion to the same order as above. An alternative and more transparent approach is first to minimize the distance between approximants and then to verify that (15) holds. This is the reverse order to the previous scheme that solves (15) which then automatically ensures that the distance between the two successive approximant is minimized.

In practice, this is implemented as follows. From (12), we see that the critical point is located at $t_c^2 = s/b_1$, i.e., $s = b_1 t_c^2$. Using only

$$p_1(t) = 1 + b_1 t^2,$$

we estimate $t_c^2 = -1/b_1$, which then yields $s = -1$. Note that this value -1 for the exponent always holds for any value of b_1. This exponent thus plays a role analog to a mean-field approximation in statistical physics. The fact that the exponent is in the present case equal to the exact value is a mere coincidence.

In the next order,

$$p_2(t) = 1 + b_1 t^2 + b_2 t^4.$$

The two approximants can be derived directly from the general formulas:

$$F_1^*(t) = \left(1 - \frac{b_1}{s_1} t^2\right)^{-s_1},$$

$$F_2^*(t) = \left[\left(1 + b_1 t^2\right)^{-2/s_2} - \frac{2b_2}{s_2} t^4\right]^{-s_2/2}.$$

We assume in addition that

$$s_1 = \frac{s_2}{2} = s, \tag{16}$$

thus eliminating a trivial dependence of the control parameter s on the approximation number k. Note that (16) is different from (14) because we use a different sequence of approximations $f_1, f_2, \ldots$. In particular, the condition (16) ensures that $F_1^*(t)$ and $F_2^*(t)$ have the same exponent/control parameter.

In constrast with the previous method of section 4.1, we first minimize the difference $F_2^*(t,s) - F_1^*(t,s)$, and then verify that (15) holds. The difference calculated at the "mean-field" threshold $t_0^2 = -1/b_1$ gives

$$D_1(s) = \left[\frac{1+s}{s}\right]^{-s} - \left(\frac{-b_2}{b_1^2\, s}\right)^{-s},$$

which is exactly zero at

$$s = -1 - \frac{b_2}{b_1^2} = -1.167.$$

The position of the critical point t_c can be recalculated from the condition $F_1^*(t_c, s) = 0$, which has a nontrivial solution at

$$t_c = \sqrt{\frac{s}{b_1}} = \sqrt{\frac{-1}{b_1}}\,\sqrt{1 + \frac{b_2}{b_1^2}} = 1.528.$$

Expanding in powers of b_2/b_1^2, we estimate $t_c \approx \sqrt{-1/b_1}(1 + b_2/2b_1^2) = 1.532$.

Thus, the renormalization scheme used to calculate t_c and K corresponds to an expansion around the mean field value $t_c^2 = 1/b_1$ and $K = 1$ in inverse powers of the dimensionless "Froude" number b_1^2/b_2 (see [46] for a definition and use of the Froude number in this context of functional renormalization). In summary, we get the predictions $t_c = 1.528$ closer to the exact value $\pi/2 = 1.5708$, and the critical exponent $K = 1.167$.

Higher-order expansion. Including the next order in $f_3(t) = f_2(t) + a_3 t^6$, inverting it, and expanding in powers of t up to t^6-terms, we obtain an expansion $p_3(t)$ for $1/f_3$:

$$p_3(t) = \sum_{k=0}^{3} b_k t^{2k},$$

with

$$b_1 = -1/2, \quad b_2 = 1/24, \quad b_3 = -1/720.$$

The two higher-order approximants can be written as follows:

$$F_2^*(t, s_2) = \left[\left(1 + b_1 t^2\right)^{-2/s_2} - \frac{2\, b_2}{s_2} t^4\right]^{-s_2/2},$$

$$F_3^*(t, s_3) = \left[\left(1 + b_1 t^2 + b_2 t^4\right)^{-3/s_3} - \frac{3\, b_3}{s_3} t^6\right]^{-s_3/3}.$$

Assume that

$$\frac{s_2}{2} = \frac{s_3}{3} = s.$$

The difference $F_3^*(t,s) - F_2^*(t,s)$ calculated at the "mean-field" critical point $t_0^2 = -1/b_1$ gives

$$D_2(s) = \left[\left(\frac{b_2}{b_1^2}\right)^{-1/s} - \frac{b_3}{s}\left(-\frac{1}{b_1}\right)^3\right]^{-s} - \left(\frac{-b_2}{b_1^2\ s}\right)^{-s},$$

which has a zero at $s = -1.024$. The position of the critical point t_c can be recalculated from the condition $1/f_3^*(t_c,s) = 0$, which has a non-trivial solution at $t_c = 1.5722$ determined from the equation

$$\left(1 + b_1 t_c^2 + b_2 t_c^4\right)^{1/s} - \frac{b_3}{s} t_c^6 = 0 \qquad (s = -1.024)\ ,$$

which wins over the "trivial solution" of $1 + b_1 t^2 + b_2 t^4 = 0$ at 1.592. Note that at order 2, from the condition $F_2^*(t_c,s) = 0$, we could only find the trivial solution $t_c^2 = 1/b_1$. It is only at higher order, starting with the order 3 discussed here, that we get corrections to the "mean-field" approximation.

To test the validity of the expansion and the strength of the corrections to the mean-field approximation, let us represent s as $s = -1 + X$, substitute it into equation $D_2(s) = 0$, and expand in powers of X, thus assuming that X is small compared to -1. Keeping only terms linear in X, X can be expressed as follows:

$$X = -\frac{b_3}{b_1 b_2}\frac{1}{1 - \ln(b_2/b_1^2)},$$

Such an expansion is justified only when $b_3/(b_1 b_2) \ll 1$ and $1 - \ln(b_2/b_1^2)$ is significantly different from zero. In our case, $b_3/(b_1 b_2) = 0.067$, $1 - \ln(b_2/b_1^2) = 2.792$ and thus $X = -0.024$ is small as expected.

Similarly, let us represent t_c^2 as $t_c^2 = -1/b_1 + C$, substitute it into the equation $F_3^*(t_c,s) = 0$, and expand in powers of C, thus assuming that C is small compared to $-1/b_1$. Keeping only the terms linear in C, we get $C = 0.458$, which leads to the value of the critical point $t_c = 1.568$ (close to 1.5722). The expression for C has a simpler structure at the mean-field point $s = -1$:

$$C = -\frac{1}{b_1}\left(\frac{b_3}{b_1\ b_2} - 1\right)\frac{1}{2 - 3\frac{b_3}{b_1\ b_2} - \frac{b_1^2}{b_2}},$$

with an estimate for the critical time given by

$$t_c \approx \sqrt{-\frac{1}{b_1}}\sqrt{1 + \left(\frac{b_3}{b_1 b_2} - 1\right)\frac{1}{2 - 3\frac{b_3}{b_1\ b_2} - \frac{b_1^2}{b_2}}} = 1.563.$$

Thus, the renormalization scheme used to calculate t_c and K corresponds to an expansion around the mean field value $t_c = 1/b_1$ and $K = 1$, in powers of two dimensionless parameters $b_3/(b_1 b_2)$ and b_2/b_1^2.

In summary, we get the predictions $t_c = 1.5722$ very close to the exact value $\pi/2 = 1.5708$ and $K = 1.024$ only 2% off the exact value 1.

We conclude that the applicability of the scheme presented in this section crucially depends on the existence of typical small parameters, while the original scheme of [8] does not have such a dependence and can be applied even if critical indices deviate strongly from the mean-field values.

4. Synthetic tests in the presence of noise

Fig. 2 shows one realization of a synthetic noisy data obtained from (3) with a multiplicative noise of variance 10^{-2}. This noisy data simulates an experiment recording a signal as a function of time or of increasing strain or stress. Our goal is to use this noisy time series up to a maximum value

away from t_c to guess using the functional renormalization method what is the critical value t_c of divergence (theoretically equal to $\pi/2 = 1.57...$).

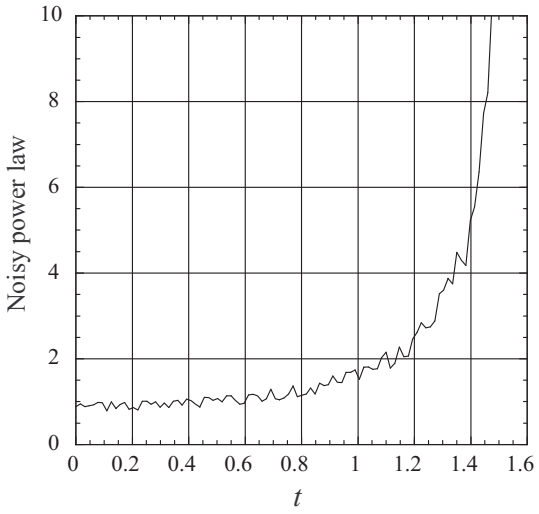

Fig. 2. Noisy data obtained from (3) with a multiplicative noise of variance 10^{-2}. The goal is to use this noisy time series up to a maximum value away from t_c to guess what is the critical value t_c of divergence (theoretically equal to $\pi/2 = 1.57...$).

Fig. 3 shows the inverse of the function in Fig. 2, as well as four other realizations, which are used in the functional renormalization scheme developed in the previous sections to predict t_c. The five different symbols shown in Fig. 3 correspond each to a single time series for a specific noise realization. The spread around the theoretical $\cos t$ formula gives a sense of the amplitude of the multiplicative noise.

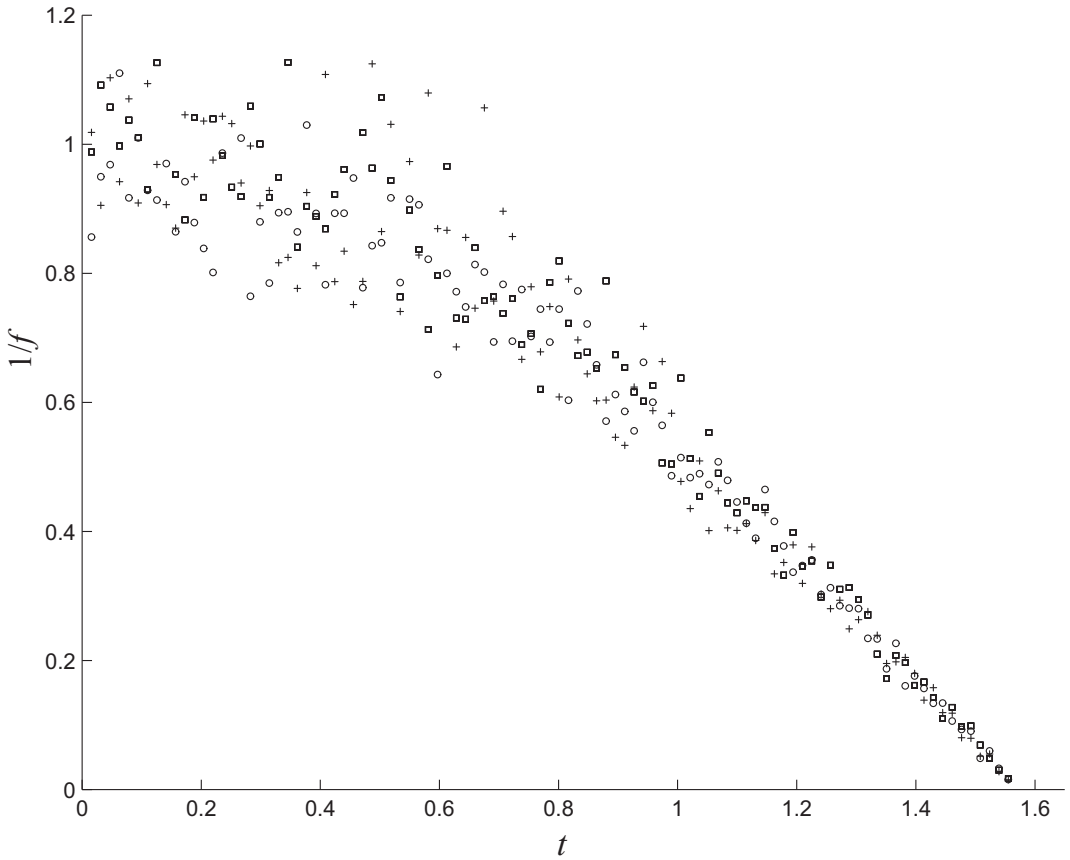

Fig. 3. The inverse of the function shown in Fig. 2 as well as four other realizations, which are used in the functional renormalization scheme developed here to predict t_c. The five different symbols shown in the figure correspond each to a single time series for a specific noise realization. The spread around the theoretical $\cos t$ formula gives a sense of the amplitude of the multiplicative noise.

Fig. 4 compares the prediction skill of our procedure described in section 4.2 to that from a direct fit with a power law, using the standard least-square fit method applied to the data without any pre-treatment. Specifically, we plot the predicted value for the critical time t_c as a function of the distance to t_c, obtained with the two schemes. In this goal, we generated 1,000 synthetic data sets using expression (3) and modifying it with a multiplicative noise of variance 10^{-3} corresponding to a standard deviation of 3.3%, i.e., with the equation $f_i(t) = [1 + \eta]/\cos t$, where η is a Gaussian white noise with variance 10^{-3}. To generate curve a) in Fig. 4, each data set was fitted by the power law equation $A(t_c - t)^{-\beta}$, with $\beta = 1$ fixed and A and t_c determined from the fit in the time interval $[0.5; T_{\rm lastpoint}]$. The thick line is the average t_c taken over the 1,000 realizations and the two thin lines are the $\pm$ one standard deviations. The curve b) in Fig. 4 is the predicted t_c obtained from our resummation technique given in section 4.2 which assumes that the exponent β is close to 1, using the coefficients b_1 and b_2 of the fit with the expansion $1 + b_1 t^2 + b_2 t^4$ to the inverse of each of the synthetic data set $f_i(t)$. The thick line is the average predicted t_c and the two thin lines are the $\pm$ one standard deviations. The horizontal line at $t_c = \pi/2$ is the exact theoretical value for the critical time. Up to very close to the critical time, our resummation method is clearly superior to the power law fit, even when knowing a priori the value of the exponent.

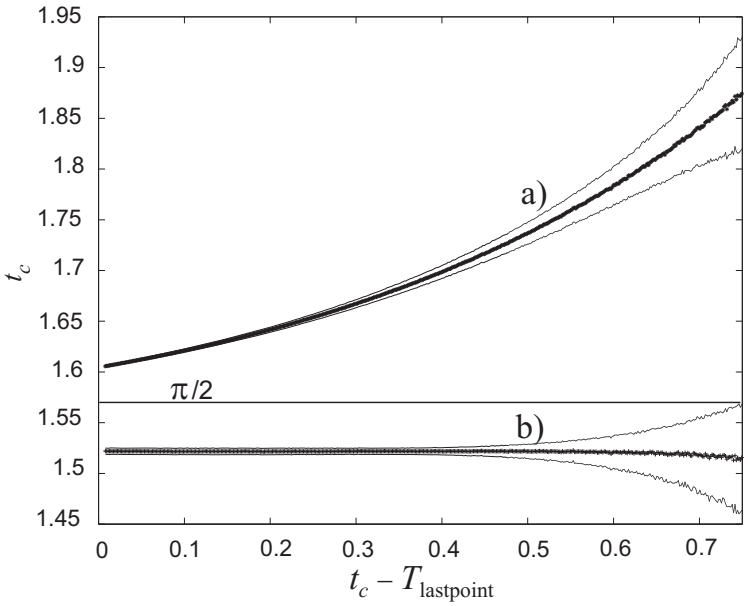

Fig. 4. The predicted value for the critical time t_c as a function of the distance to t_c, obtained with different schemes, in order to evaluate the value of the resummation procedures proposed here. In this goal, 1,000 synthetic data sets were generated using expression (3) and modifying it with a multiplicative noise of variance 10^{-3} corresponding to a standard deviation of 3.3%, i.e., with the equation $f_i(t) = [1+\eta]/\cos t$, where η is a Gaussian white noise with variance 10^{-3}. To generate curve a), each data set was fitted by the power law equation $A(t_c - t)^{-\beta}$, with $\beta = 1$ fixed and A and t_c determined from the fit in the time interval $[0.5; T_{\rm lastpoint}]$. The thick line is the average t_c taken over the 1,000 realizations and the two thin lines are the $\pm$ one standard deviations. The curve b) is the predicted t_c obtained from our resummation technique given in section 4.2 which assumes that the exponent β is close to 1, using the coefficients b_1 and b_2 of the fit with the expansion $1+b_1t^2+b_2t^4$ to the inverse of each of the synthetic data set $f_i(t)$. The thick line is the average predicted t_c and the two thin lines are the $\pm$ one standard deviations. The horizontal line at $t_c = \pi/2$ is the exact theoretical value for the critical time. Up to very close to the critical time, our resummation method is clearly superior to the power law fit, even when knowing a priori the value of the exponent.

Fig. 5 compares the prediction skill of the Yukalov-Gluzman method used in section 4.1 to that of a direct power law fit. Again, 1,000 synthetic time series were generated with multiplicative noise of variance 10^{-3}. The curve a) of Fig. 5 is obtained by using the general resummation method of section 4.1 which does not assume any specific value of the exponent β. We first fit the inverse of each synthetic data set with a parabolic expression $1 + b_1 t^2 + b_2 t^4$ and use these coefficients b_1 and b_2 to obtain our prediction t_c. The two thin lines are the $\pm$ one standard deviations. The curve b) in Fig. 5 is obtained by fitting each data set by the power law equation $A(t_c - t)^{-\beta}$, where A, β and

t_c are all three free parameters determined from the fit in the time interval $[0.5; T_{\text{lastpoint}}]$. The thick line is the average t_c taken over the 1,000 realizations and the two thin lines are the $\pm$ one standard deviations. The horizontal line at $t_c = \pi/2$ is the exact theoretical value for the critical time. Note the striking superiority of our resummation method over a direct power law fit.

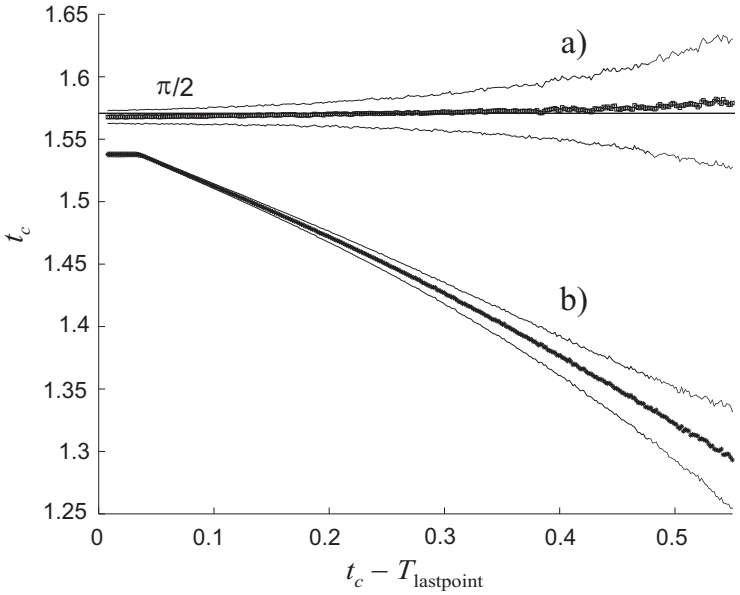

Fig. 5. Same as Fig. 4 with 1,000 synthetic time series with multiplicative noise of variance 10^{-3}, and with different prediction schemes. The curve a) is obtained by using the general resummation method of section 4.1 which does not assume any specific value of the exponent β. We first fit the inverse of each synthetic data set with a parabolic expression $1 + b_1 t^2 + b_2 t^4$ and use these coefficients b_1 and b_2 to obtain our prediction t_c. The two thin lines are the $\pm$ one standard deviations. The curve b) is obtained by fitting each data set by the power law equation $A(t_c - t)^{-\beta}$, where A, β and t_c are all three free parameters determined from the fit in the time interval $[0.5; T_{\text{lastpoint}}]$. The thick line is the average t_c taken over the 1,000 realizations and the two thin lines are the $\pm$ one standard deviations. The horizontal line at $t_c = \pi/2$ is the exact theoretical value for the critical time. Note the striking superiority of our resummation method over a direct power law fit.

Fig. 6 is the same as Fig. 4 but with a larger multiplicative noise of variance 10^{-2}. Fig. 7 is the same as Fig. 5 but with a larger multiplicative noise of variance 10^{-2}.

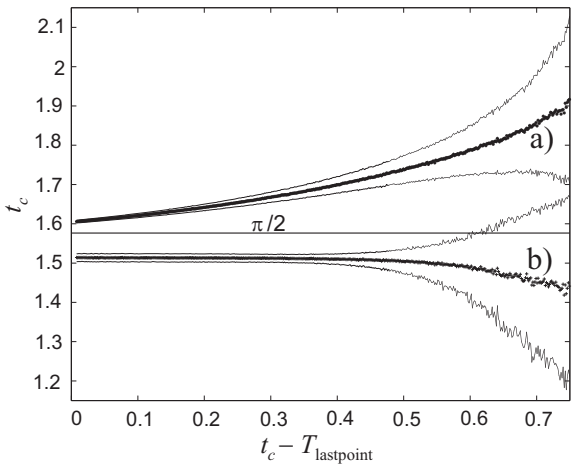

Fig. 6. Same as Fig. 4 but with a multiplicative noise of variance 10^{-2}.

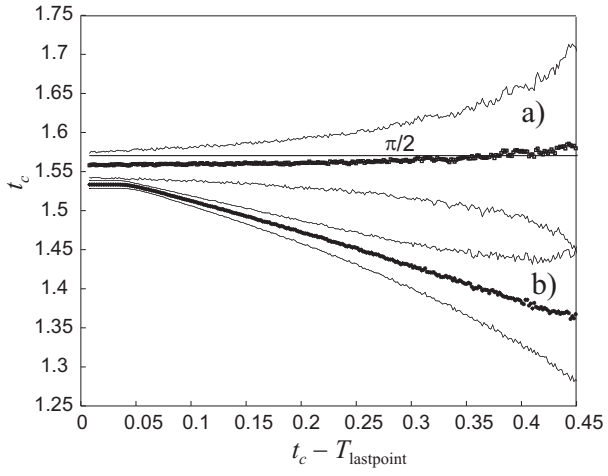

Fig. 7. Same as Fig. 5 but with a multiplicative noise of variance 10^{-2}.

5. Concluding remarks

We have tested two methods for the prediction of the critical time of a singular power law behavior and tested their prediction skills against the direct determination by a power law fit. Our analysis and the numerical tests convincingly demonstrate the value of our approach which provides significant improved forecasting skills. Our tests have however been restricted to a an important from a physical viewpoint but still special case of a function which admits an expansion with only even powers of t. The most general situation contains also odd powers of t which complicates the situation. We intend to report progress in this general case in a forthcoming publication.

Finally, we wish to comment upon a conceptual understanding of the role of the exponent s used as control functions in the functional renormalization schemes used here. Yukalov and Gluzman [38] first noticed that their functional renormalization frameworks allowed them to propose a novel physical understanding of critical exponents as being directly related to limits of control functions at the critical point. In other words, they appear as physical analogs of the rather abstract mathematical objects given by the control functions. A scale invariant formulation using logarithmic variables allows us to understand this rather surprising observation: critical exponents can be seen to be determined by the initial conditions of an operator of the group of the symmetry of scale invariance [45]. Indeed, a power law function $\varphi(r)$ of the distance $r \equiv t_c - t$ to the critical point, has the property of scale invariance which reads

$$\varphi(\lambda r) = \lambda^{\alpha}\varphi(r), \tag{17}$$

where λ is an arbitrary magnification factor and α is a critical exponent. This equation means that the field $\varphi(r)$ is invariant under the homothetic mapping $r \to \lambda r$; $\varphi \to \lambda^{-\alpha}\phi$. Expression (17) can be transformed by picking up an arbitrary reference field φ_0 and an arbitrary reference parameter r_0 and introducing the log-variables $U = \ln(\varphi/\varphi_0), s = r/r_0, U(0) = \ln(\varphi(r_0)/\varphi_0), U(s) - U(0) = \alpha s$. In these variables, equation (17) can also be written:

$$\begin{aligned} U(s) &= U(s+\mu) + g(\mu), \\ g(\mu) &= U(0) - U(\mu), \qquad \text{for any } \mu. \end{aligned} \tag{18}$$

Reciprocally, any regular function obeying (18) is necessarily of the shape $U(s) - U(0) = \alpha s$, where

$$\alpha = U(1) - U(0)$$

is an arbitrary parameter selected by the initial conditions! The message here is not that a power-like function (17) is determined by its values at two arbitrary points, which is obvious, but that an exponent α can be seen as a boundary condition in the log-variables. Since boundary conditions are usually the place where forces/controls can be applied, we believe that this sheds some light on the status of critical exponents identified by Yukalov and Gluzmann as limits of control functions.

REFERENCES

1. *Reichhardt T.* Rocket failure leads to grounding of small US satellites // Nature. 1996. Vol.384. P.99.
2. *Mogi K.* Some features of recent seismic activity in and near Japan 2: Activity before and after great earthquakes // Bull. Eq. Res. Inst. Tokyo Univ. 1969. Vol.47. P.395–417.
3. *Mogi K.* Earthquake prediction research in Japan // J. Phys. Earth. 1995. Vol.43. P.533–561.
4. *Andersen J.V., Sornette D., Leung K.-T.* Tri-critical behavior in rupture induced by disorder // Phys. Rev. Lett. 1997. Vol.78. P.2140–2143.
5. *Sornette D., Andersen J.-V.* Scaling with respect to disorder in time-to-failure // Eur. Phys. J. 1998. Vol.B1. P.353–357.
6. *Vere-Jones D.* Statistical theories of crack propagation // Math. Geology. 1977. Vol.9. P.455–481.
7. *Allègre C.J., Le Mouel J.L., Provost A.* Scaling rules in rock fracture and possible implications for earthquake predictions // Nature. 1982. Vol.297. P.47–49.
8. *Sornette D.* Critical Phenomena in Natural Sciences, Chaos, Fractals, Self-organization and Disorder: Concepts and Tools. Springer Series in Synergetics, 2000, 434 p.
9. *Keilis-Borok V.* The lithosphere of the Earth as a large nonlinear system // Geophys. Monogr. Ser. 1990. Vol.60. P.81–84.

10. *Shnirman M.G.* Dynamical hierarchical model of defect formation // Computational Seism. 1987. Vol.20. P.87–95; English translation, 1988. P.85–92.
11. *Shnirman M.G., Blanter E.M.* Self-organized criticality in a mixed hierarchical system // Phys. Rev. Lett. 1998. Vol.81. P.5445–5448.
12. *Sornette D., Vanneste C.* Dynamics and memory effects in rupture of thermal fuse networks // Phys. Rev. Lett. 1992. Vol.68. P.612–615.
Vanneste C., Sornette D. Dynamics of rupture in thermal fuse models // J. Phys. I France. 1992. Vol.2. P.1621–1644.
13. *Lamaignère L. Carmona F., Sornette D.* Experimental realization of critical thermal fuse rupture // Phys. Rev. Lett. 1996. Vol.77. P.2738–2741.
14. *Bradley R.M., Wu K.* Dynamic fuse model for electromigration failure of polycrystalline metal films // Phys. Rev. E. 1994. Vol.50. P.R631–R634.
15. *Anifrani J.-C., Le Floc'h C., Sornette D., Souillard B.* Universal log-periodic correction to renormalization group scaling for rupture stress prediction from acoustic emissions // J. Phys. I France. 1995. Vol.5. P.631–638.
16. *Sornette D.* Discrete scale invariance and complex dimensions // Phys. Reports. 1998. Vol.297. P.239–270.
17. *Sahimi M., Arbabi S.* Scaling laws for fracture of heterogeneous materials and rocks // Phys. Rev. Lett. 1996. Vol.77. P.3689–3692.
18. *Ray P., Date G.* Spatial scaling in fracture propagation in dilute systems // Physica A. 1996. Vol.229. P.26–35.
19. *Garcimartin A., Guarino A., Bellon L., Ciliberto S.* Statistical properties of fracture precursors // Phys. Rev. Lett. 1997. Vol.79. P.3202–3205.
Guarino A., Garcimartin A., Ciliberto S. // Eur. Phys. J. 1998. Vol.B6. P.13.
Guarino A., Ciliberto S., Garcimartin A. // Europhysics Lett. 1999. Vol.47. P.456.
20. *Johansen A., Sornette D.* Critical ruptures, Critical ruptures // Eur. Phys. J. 2000. Vol.B18. P.163–181.
21. *Sornette D., Sammis C.G.* Complex critical exponents from renormalization group theory of earthquakes: Implications for earthquake predictions // J. Phys. I France. 1995. Vol.5. P.607–619.
22. *Sykes L.R., Jaumé S.* Seismic activity on neighboring faults as a long-term precursor to large earthquakes in the San Francisco Bay Area // Nature. 1990. Vol.348. P.595–599.
23. *Bufe C.G., Varnes D.J.* Predictive modelling of the seismic cycle of the greater San Francisco bay region // J. Geophys. Res. 1993. Vol.98. P.9871–9883.
24. *Huang Y., Saleur H., Sammis C.G., Sornette D.* Precursors, aftershocks, criticality and self-organized criticality // Europhys. Lett. 1998. Vol.41. P.43–48.
25. *Bowman D.D., Ouillon G., Sammis C.G., Sornette A., Sornette D.* An Observational test of the critical earthquake concept // J. Geophys. Res. 1998. Vol.103. P.24359–24372.
26. *Jaumé S.C., Sykes L.R.* Evolving towards a critical point: A review of accelerating seismic moment/energy release prior to large and great earthquakes // Pure and Applied Geophysics. 1999. Vol.155. P.27–305.
27. *Ouillon G., Sornette D.* The critical earthquake concept applied to mine rockbursts with time-to-failure analysis // Geophys. J. Inter. 2000. Vol.143. P.454–468.
28. *Voight B.* A method for prediction of volcanic eruptions // Nature. 1998. Vol.332. P.125–130.
Cornelius R.R., Voight B. Graphical and PC-Software analysis of volcano eruption precursors according to the materials failure forecast method (FFM) // J. Volcanol. Geotherm. Res. 1995. Vol.64. P.295–320.
29. *Voight B.* A relation to describe rate-dependent material failure // Science. 1989. Vol.243. P.200–203.
30. *Johansen A., Sornette D., Wakita H., Tsunogai U., Newman W.I., Saleur H.* Discrete scaling in earthquake precursory phenomena: evidence in the Kobe earthquake, Japan // J. Phys.I France. 1996. Vol.6. P.1391–1402.
31. *Yukalov V.I.* Statistical mechanics of strongly non-ideal systems // Phys. Rev. A. 1990. Vol.42. P.3324–3334.
32. *Yukalov V.I.* Method of self-similar approximations // J. Math. Phys. 1991. Vol.32. P.1235–1239.
33. *Yukalov V.I.* Stability conditions for method of self-similar approximations // J. Math. Phys. 1992. Vol.33. P.3994–4001.
34. *Yukalov V.I., Yukalova E.P.* Higher orders of self-similar approximations for thermodynamic potentials // Physica A. 1994. Vol.206. P.553–580.
35. *Yukalov V.I., Yukalova E.P.* Temporal dynamics in perturbation theory // Physica A. 1996. Vol.225. P.336–362.
36. *Gluzman S., Yukalov V.I.* Algebraic self-similar renormalization in the theory of critical phenomena // Phys. Rev. E. 1997. Vol.55. P.3983–3999.
37. *Yukalov V.I, Gluzman S.* Self-Similar Bootstrap of Divergent Series // Phys. Rev. E. 1997. Vol.55. P.6552–6570.
38. *Yukalov V.I, Gluzman S.* Critical Indices as Limits of Control Functions // Phys. Rev. Lett. 1997. Vol.79. P.333–336.
39. *Yukalov V.I, Gluzman S.* Self-similar exponential approximants // Phys. Rev. E. 1998. Vol.58. P.1359–1382.
40. *Gluzman S., Yukalov V.I.* Unified Approach to Crossover Phenomena // Phys. Rev. E. 1998. Vol.58. P.4197–4209.
41. *Yukalov V.I., Gluzman S.* Self-Similar Crossover in Statistical Physics // Physica A. 1999. Vol.273. P.401–415.
42. *Yukalov V.I., Yukalova E.P., Gluzman S.* Self-Similar Interpolation in Quantum Mechanics // Phys. Rev. A. 1998. Vol.58. P.96–115.
43. *Rabotnov Yu. N.* Elements of hereditary solid mechanics. Moscow: Mir, 1980, 387 p.
44. *Gluzman S., Sornette D.* Self-Consistent Theory of Rupture by progressive diffuse damage, submitted to Physical Review E, preprint at $http://arXiv.org/abs/cond-mat/0010207$, 2000.
45. *Dubrulle B.* Finite size scale invariance // Eur. Phys. J. B. 2000. Vol.14. P.757–771.
46. *Andersen J.V., Gluzman S., Sornette D.* Fundamental Framework for Technical Analysis // Eur. Phys. J., B. 2000. Vol.14. P.579–601.